



An Intelligent Machine Learning-Based Protection of AC Microgrids Using Dynamic Mode Decomposition

M. Dodangeh* and N. Ghaffarzadeh*(C.A.)

Abstract: An intelligent strategy for the protection of AC microgrids is presented in this paper. This method was halving to an initial signal processing step and a machine learning-based forecasting step. The initial stage investigates currents and voltages with a window-based approach based on the dynamic decomposition method (DDM) and then involves the norms of the signals to the resultant DDM data. The results of the currents and voltages norms are applied as features for a topology data analysis algorithm for fault type classifying in the AC microgrid for fault location purposes. The Algorithm was tested on a microgrid that operates with precision equal to 100% in fault classification and a mean error lower than 20 m when forecasting the fault location. The proposed method robustly operates in sampling frequency, fault resistance variation, and noisy and high impedance fault conditions.

Keywords: AC Microgrid, Fault Location and Classification, Intelligent Protection, Machine Learning, TDA-ML.

1 Introduction

THE major aim of power system protection strategies is to save the system safely with minimum failures and outages. To accomplish so, protection methods try to separate the faulted parts of the system only. To do this mission effectively, protection devices and algorithms must have high precision for fault detection, classifying, and location. The time which spends on protection tools to employ correctional acts has been reduced especially in recent years. These results have been achievable by presenting time-domain protection algorithms like the traveling waves idea, higher sampling frequency of the signals measuring, and developed strategies to extract the processed signals' information. The most famous of these strategies is the discrete wavelet transform (DWT) [4-5] and mathematical morphology (MM) [6].

Study on distribution grids protection has also offered the advantages of using deep learning (DL) and machine learning (ML) manners in the missions of fault location and fault classification [7].

Deep learning and DWT-based approaches mixed for protection usages such as fault location, detection, and classification are presented [8-12]. For MM approaches, this has also been explored [13, 20]. Other than [12], these methods generally need signals of at least a couple of milliseconds to be able to achieve the required protection plan. However, the result in [12] illustrated that even in 0.1 ms window of a combined DWT and ML method can classify and locate faults in a power grid. Ref [14] investigates the power quality disturbances such as a single line to ground and three phase faults using the dynamic mode decomposition. The dynamic decomposition method (DDM) is a suitable instrument for network signal processing in disturbances of faults [14]. The approach proposed in [14] showed the real value of the DDM eigenvalues differences in faulted cases. This research suggests an intelligent method to classify and locate faults based on the combination of the DDM technique in [14] and ML.

In this study, DDM is used to calculate the eigenvalues of the system. The suggested method initially receives time signals related to the DDM eigenvalues of the voltages and current signals. Then

Iranian Journal of Electrical and Electronic Engineering, 2022.
Paper first received 31 May 2022, revised 03 September 2022, and accepted 12 September 2022.

* The authors are with the Department of Electrical Engineering, Imam Khomeini International University, Qazvin 3414896818, Iran.
E-mails: mostafadodangeh@edu.ikiu.ac.ir and ghaffarzadeh@eng.ikiu.ac.ir.

Corresponding Author: N. Ghaffarzadeh.
<https://doi.org/10.22068/IJEEE.18.4.2544>

ℓ_p -norms are employed to get metrics from the DDM signals which are then used as the features of an ML algorithm, which was selected to be a topology data analysis (TDA). The paper illustrates the importance of the features for the classification and location missions. The method is tested in the distribution system as [12]. The main contribution of the presented algorithm was that the mean forecast error for the fault location task was decreasing from 62% to 21% compared with [12]. Because the results in [12] show an accuracy of 100%, those results cannot be improved but were matched by the proposed method.

The rest of the paper is organized as follows. The power system used in this work is presented in Section 2. The algorithm of fault location and classification with DDM and Topological data analysis (TDA) is presented in Section 3. The evaluation of the proposed strategy in the test system is illustrated in Section 4. The performance of this approach is presented in Section 5.

2 The Test AC Microgrid

The test AC microgrid is illustrated in Fig. 1. This AC microgrid is connected to a network and several renewable power generations consist of solar panels and wind turbines. This network supplies the 400 kVA loads with different-length 11 kV and 0.4 kV lines. The main network is connected to the microgrid by a 63/11 kV voltage level transformer. This network's data is

presented in the appendix.

This grid's studied faults included single phase to ground (AG, BG, CG), phase to phase (AB, AC, BC), double phase to ground (ABG, ACG, BCG), three-phase (ABC), and three phase to ground (ABCG).

The fault resistances values are: 0.01, 0.5, 2, 5, 10, 25, and 50 Ω . It also equals 500 and 1000 Ω to investigate the high impedance fault conditions. One thousand various faults are simulated in this paper. This microgrid was simulated in PSCAD/EMTDC.

The currents and voltages of the network for various faults with various resistances are measured. The three-phase currents and three-phase voltage signals are shown in Figs. 2 and 3 for a sample SLG (CG) fault condition which is simulated in the line FA of the test microgrid. The fault occurred at 2 milliseconds between phase C and ground. These signals take from simulations of the system in Fig. 1 but polluted with Gaussian noise. These signals have a signal-to-noise ratio (SNR) of 35%, which is the level of noise applied in this study. According to Fig. 2, the faulted phase current increased after fault time. Moreover, according to Fig. 3, the voltage of faulted phase is decreased and the voltage of other phases is increased. Furthermore, the currents and voltages signals of a three-phase (ABC) fault condition on the FA line are shown in Fig. 4 and Fig. 5. The three-phase short circuit fault occurred at 2 milliseconds. According to Fig. 4, the currents of all phases increased after fault occurrence time.

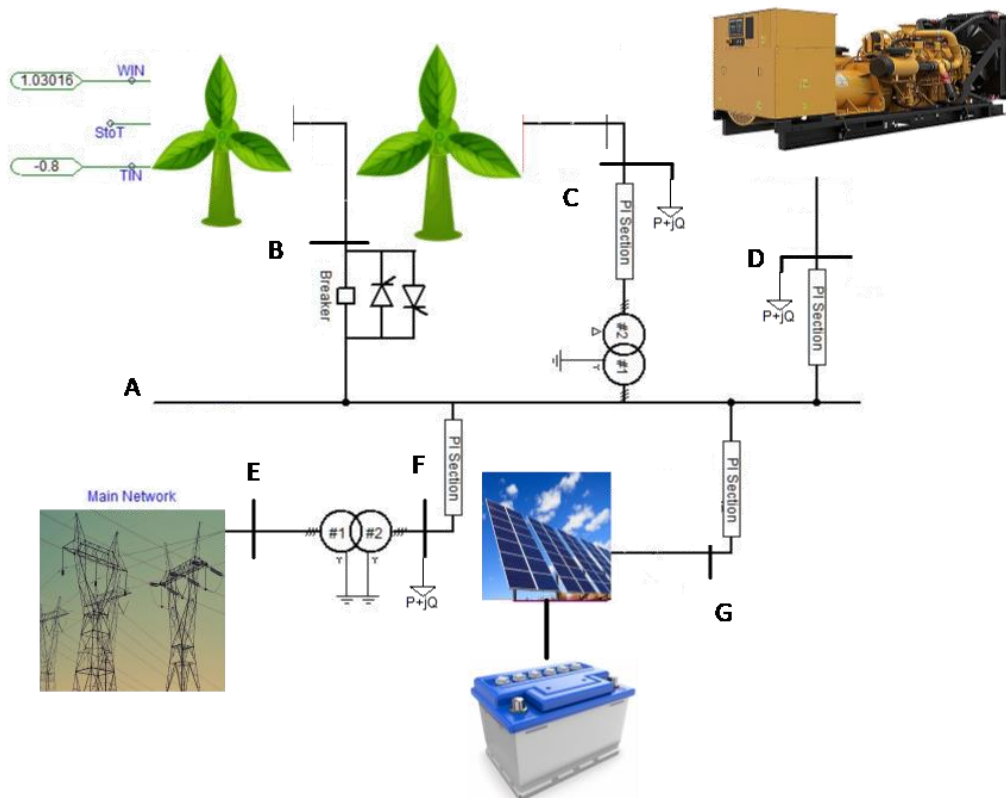


Fig. 1 AC test microgrid.

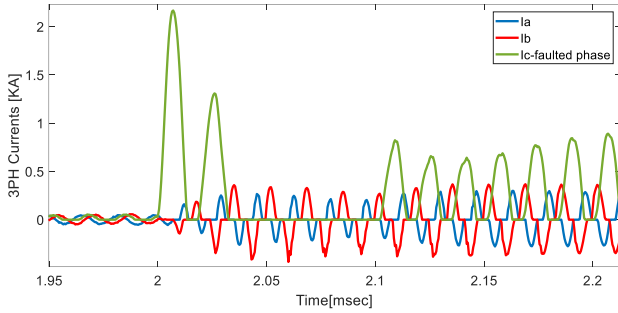


Fig. 2 The three-phase currents in an SLG fault condition.

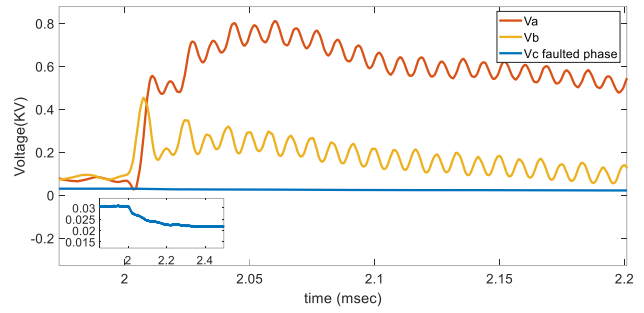


Fig. 3 The voltage signals for an SLG fault condition.

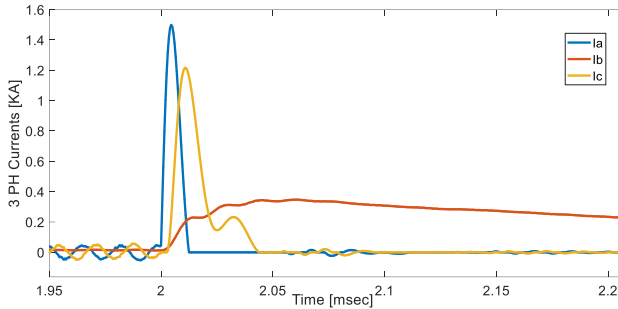


Fig. 4 The current signals in an (ABC) fault condition.

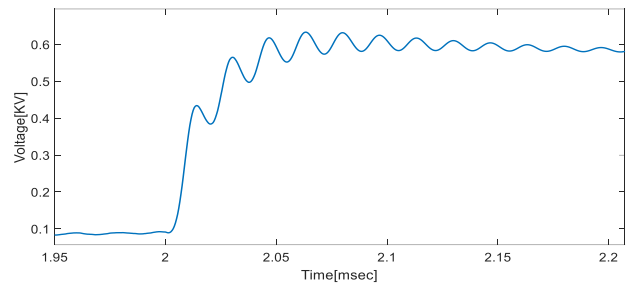


Fig. 5 The voltage (RMS) signal in an (ABC) fault condition.

3 Protection Strategy

In this section, the suggested algorithm for ac microgrid protection is presented. The methodology uses a window of 100 μ s of voltage and current measures from the microgrid by 50 μ s coming before and 50 μ s coming after the fault detection. These data were studied with the DDM and norms-based metrics. The data generated in the metrics step is utilized to train an intelligent algorithm for fault location and another for fault classification.

3.1 The Dynamic Decomposition Method

The eigenvalues and eigenvectors of the system are calculated by the dynamic decomposition method. DDM is a system dynamics estimation method from measured signals [15], [16]. This algorithm calculates the most suitable linear dynamics of the system for which the information is captured even if that system is nonlinear. The Koopman (or composition) operator which approximates by DDM is a linear, infinite-dimensional operator that can represent nonlinear systems on a (Hilbert) space of measure parts of its condition. The Koopman operator has the ability to illustrate nonlinear dynamics by existing as an infinite-dimensional operator, even though it is linear [17].

The Koopman operator can be a DDM that identifies the finite-dimensional linear system's eigenvectors (values) that can be considered as estimates of the infinite-dimensional Koopman operator. Furthermore, The DDM is a technique of dimension reduction that, at its core, the singular value decomposition is used. Shown a sequential set of measures, $\{v_1, v_2, \dots, v_n\}$ where $v_i \in \mathbb{R}^n$ and $\forall i = 1 \dots n$, taken from a system at

standard intervals, DDM calculates

$$v_{j+1} = Av_j \tag{1}$$

which is a linear technique of representation that catches the dynamics present in the set of the measurements. The DDM input formally is a measurement set of signals and two following matrices are outputs:

$$\Theta = \begin{bmatrix} \vdots & \vdots & \dots & \vdots & \vdots \\ \theta_1 & \theta_2 & \dots & \theta_{r-1} & \theta_r \\ \vdots & \vdots & \dots & \vdots & \vdots \end{bmatrix} \tag{2}$$

$$N = \begin{bmatrix} v_1 & 0 & \dots & 0 & 0 \\ 0 & v_2 & \dots & \vdots & \vdots \\ \vdots & 0 & \ddots & 0 & \vdots \\ \vdots & \vdots & \dots & v_{r-1} & 0 \\ 0 & 0 & \dots & 0 & v_r \end{bmatrix} \tag{3}$$

N includes the system's eigenvalues and Θ is the matrix that corresponds right eigenvectors. Importantly that the r is the relevant dimension of the DDM technique which is determined by the user. ($r \leq n$ and for $r = n$ the DDM has not reduced the dimension). It has been explained that DDM is a capable approach for power systems and their disturbances signals studies [14]. In [14] a window-based algorithm used the DDM to power network signals distortion detection due to events in the grid. The supplementary information about the DDM technique is in [15, 16].

The dimension of the outputs of the DDM technique is determined to be 3 ($r = 3$). Currents set, voltages set, and a set with both currents and voltages are assumed as input signals and analyzed at once. Before using the

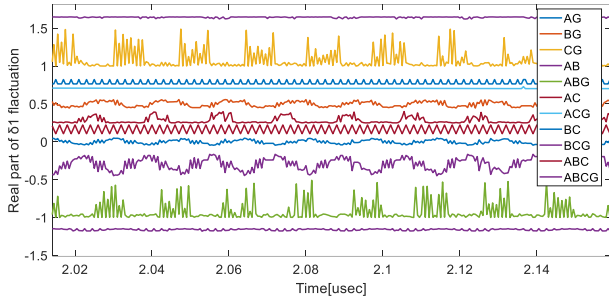


Fig. 6 Fluctuations of the eigenvalue δ_1 for each fault type.

signal of currents and voltage by the DDM method, the signals were normalized for the input of the DDM in this latter case.

The first DDM eigenvalue's real part, δ_1 is illustrated in Fig. 6 for each type of fault. The data of a 100 μ s window around the fault beginning time was utilized to obtain these effects of the measurements in Fig. 2. This figure displays that δ_1 fluctuates happened after the fault occurrence time, for all DDM window lengths assumed.

3.2 Signal Norms

The ℓ_p -norm defines for one-dimensional discrete signal in \mathbb{R}^n

$$\|v\|_q = \sqrt[q]{\sum_{j=1}^n |v_j|^q} \quad \forall 1 \leq q \leq \infty \quad (4)$$

This function executes $\mathbb{R}^n \rightarrow \mathbb{R} \geq 0$, in which $\mathbb{R} \geq 0$ is the set of non-negative parts of real number sets.

For $q = 1$, (4) describes the taxicab norm, for $q = 2$, Eq. (4) represents the Euclidean norm (energy of the signal), and when $q = \infty$, (4) describes the infinity norm. These norms have the following property

$$\|v\|_\infty \leq \|v\|_2 \leq \|v\|_1 \quad (5)$$

This study uses the 1, 2, and ∞ norms which are defined by

$$\|v\|_1 = \sum_{j=1}^n |v_j| \quad (6)$$

$$\|v\|_2 = \sqrt{\sum_{j=1}^n |v_j|^2} \quad (7)$$

$$\|v\|_\infty = \max_{1 \leq j \leq n} |v_j| \quad (8)$$

The norms in this study are applied to the signals received from the DDM method such as those shown in Fig. 4 as a method to encapsulate their inherent data. Fig. 7 displays a sample of this method for the 1-norm of δ_1 as a function of the fault location for a single phase fault condition that emphasizes the changes due to the fault resistance variation.

3.3 Fault Detection

According to Sections 3.1 and 3.2, fluctuations of the

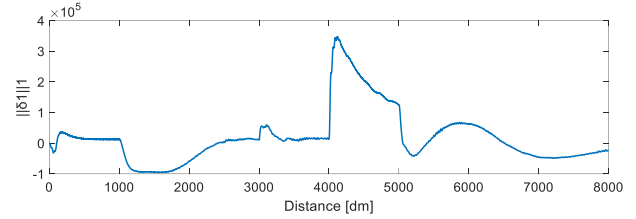


Fig. 7 Fluctuations of the eigenvalue δ_1 for each fault type.

norm of δ_1 used for fault detection.

3.4 TDA-ML for Fault Location and Classification

Topological data analysis (TDA) is a new emergent domain that aims to find topological hidden data of a dataset. TDA methods have been employed to design filters and topological descriptors to enhance Machine Learning (ML) approaches. This paper applies a method of machine learning that used TDA instantly to multi-class classification issues. The used algorithm creates a filtered simplicial complex on the dataset. Persistent Homology (PH) is used to conduct the sub-complex selection of unlabeled points to obtain the label with the majority of votes from marked near points.

Using the simulation setup described in part 2 for the microgrid in Fig. 1 creates 8000 various fault conditions. The current, voltage, and a mixture of current and voltage for each case are studied with DDM, and measures are created by the abovementioned norms in Part 2. The conditions which are simulated for each case, are as follows.

- Three measurements (voltages, currents, and voltage and currents together).
- Real part of the three eigenvalues of DDM.
- Five sampling frequencies (500, 1000, 2000, 5000, and 20000 Hz).
- Five window sizes (100, 200, 400, 800, and 1000 points).
- Five quantities of fault resistance.
- Five amounts of SNR (10, 20, 35, 50, and 60 percent).
- Three norms (1, 2, and ∞ -norm).

These amounts are employed as features for a TDL-based ML as the chosen approach in this study for fault location and classification duties.

The suggested TDA-based strategy was more suitable than the KNN and weighted version of KNN. It acts competitively with Random Forest baseline and Local SVM classification methods in balanced datasets, and it has better performance than all baseline approaches of classification involved and minority categories.

According to the abovementioned sections, the flowchart of the proposed intelligent algorithm is illustrated in Fig. 8. The voltage and current sets sampled from the network applied to DDM (1)-(3) to estimate the δ_1 . The δ_1 norms are calculated by (6)-(8). The norms of the δ_1 applied to TDA-ML-based fault location and classification algorithm.

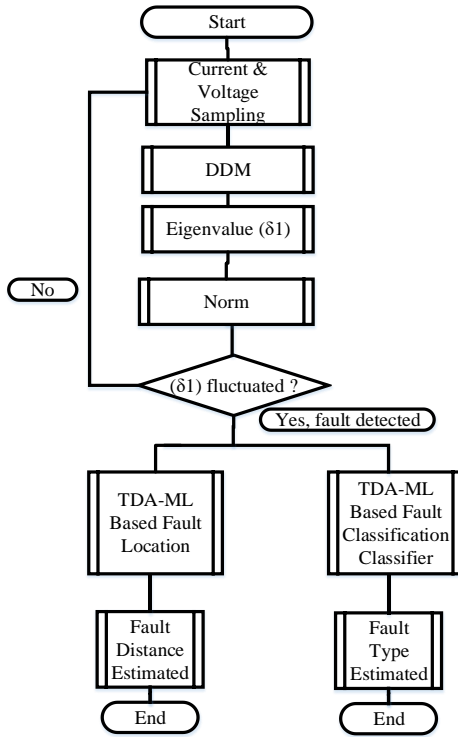


Fig. 8 proposed method flowchart.

4 Results in the Test System

This section illustrates the results of employing the TDA-ML-based fault location and classification algorithm, which is presented in part III, to a dataset of simulated faults data taken from the test microgrid in Fig. 1. In this study two independent TDA-ML are generated, one for the fault-location duty and the other for the classification aim. 64 percent of the 8000 simulated cases were used for the training. The 1280 cases created the validation set and 1600 fault conditions for the test set.

4.1 Fault Classification Task

The goal of this duty is to identify the occurred fault type, either SLG, DL, DLG, 3L, or 3LG. The TDA-ML obtained in this study was learned by the abovementioned features for each of the 6400 simulation fault conditions that were marked consequently. The performance of the TDA-ML classification method on the testing dataset is:

- Accuracy equal to 100%.
- Recall 100%.
- F-score equal to 100%.
- Precision equal to 100%.

These performances are equal to the results of [12] which the initial processing step was based on the DWT and the noise-less signals. Furthermore, this study utilized the TDA-ML's feature importance for classifying. Fig. 9 shows the 20 characteristics that are important for the TDA-ML classifier. The TDA algorithm is utilized to calculate the feature importance

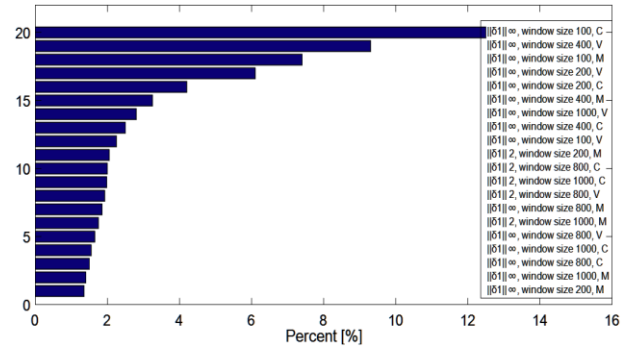


Fig. 9 Feature importance for fault classification.

Table 1 The mean error and standard deviation.

Method	Ref. [12]	Suggested algorithm
Deviation	34.77	20.23
Mean error	62.95	21.25

from different-norm of δ_1 with various window sizes. This successive method did the feature importance and feature selection by correlation analysis. The results in Fig. 9 show these factors employ both the δ_1 infinity norm and 2-norm. In this figure, C, V, and M stand for currents, voltages, and mixed signals respectively. Furthermore, Fig. 9 illustrate that all sizes of window and signals are used in the classification mission. The TDA-ML method discovers valuable details at various DDM resolutions.

4.2 Fault Location Task

The purpose of this duty is to identify the occurred fault distance. This is a regression assignment that was approached by another TDA-ML trained by the same type of dataset that the classifier was trained in. The major difference is that the labels in this problem are the fault distance. The network of TDA-ML is defined by a group of variables which is hyperparameters. These hyperparameters define important items like the minimum number of leaves. These items finally determine the TDA-ML's performance.

This research completes randomized search cross-validation to determine the most suitable group of parameters for the fault-location mission among a big dataset of candidates. The fault distance forecasting with the TDA-ML trained in this paper has the mean error and legal deviation illustrated in Table 1. This table also shows the same parameters for [12]. This table represents that the suggested method has decreased about 66% of the average error and around 42% of the legal partition [12].

The 20 most important factors for the fault location regression are presented in Fig. 10. Alike the classifier results, the results of Fig. 10 say that the selected elements are associated with the real part eigenvalue (δ_1), 2-norm, and the infinity norm. Additionally, these features are based on the currents, and voltages but not in the case that mixes them together.

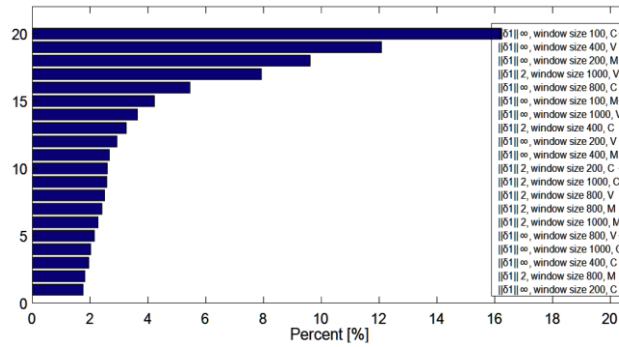


Fig. 10 Feature importance for fault location.

Table 2 Results of fault location and classification method.

Simulated Fault				Estimated fault sampling frequency										
Type	Line	SNR [%]	Resistance [Ω]	500		1000		2000		5000		20000		
				Location [%]	Type	Location [%]	Type	Location [%]	Type	Location [%]	Type	Location [%]	Type	
AG	AB	10	50	25	AG	26	AG	24	AG	27	AG	23	AG	25
	AC	30	25	40	AG	39	AG	41	AG	39	AG	40	AG	41
	FA	60	5	65	AG	63	AG	63	AG	65	AG	66	AG	64
	AD	70	0.5	15	AG	16	AG	15	AG	16	AG	14	AG	16
	AE	50	100	90	AG	92	AG	92	AG	88	AG	92	AG	91
BG	AB	10	50	25	BG	24	BG	25	BG	27	BG	24	BG	26
	AC	30	25	40	BG	41	BG	42	BG	40	BG	41	BG	39
	FA	60	5	65	BG	67	BG	64	BG	63	BG	66	BG	66
	AD	70	0.5	15	BG	15	BG	16	BG	14	BG	15	BG	15
CG	AB	10	50	25	CG	26	CG	23	CG	27	CG	24	CG	25
	AC	30	25	40	CG	40	CG	41	CG	38	CG	41	CG	42
	FA	60	5	65	CG	65	CG	63	CG	66	CG	63	CG	67
	AD	70	0.5	15	CG	14	CG	15	CG	15	CG	15	CG	14
	AE	50	100	90	CG	93	CG	90	CG	91	CG	92	CG	89
AB	AB	10	50	25	AB	27	AB	25	AB	25	AB	26	AB	26
	AC	30	25	40	AB	39	AB	40	AB	43	AB	39	AB	39
	FA	60	5	65	AB	65	AB	65	AB	65	AB	63	AB	63
	AD	70	0.5	15	AB	16	AB	15	AB	15	AB	16	AB	16
	AE	50	100	90	AB	88	AB	90	AB	89	AB	92	AB	92
AC	AB	10	50	25	AC	25	AC	25	AC	24	AC	24	AC	27
	AC	30	25	40	AC	41	AC	41	AC	41	AC	41	AC	39
	FA	60	5	65	AC	64	AC	64	AC	63	AC	67	AC	65
	AD	70	0.5	15	AC	16	AC	16	AC	15	AC	15	AC	16
	AE	50	100	90	AC	91	AC	91	AC	92	AC	92	AC	88
BC	AB	10	50	25	BC	26	BC	26	BC	25	BC	26	BC	27
	AC	30	25	40	BC	39	BC	39	BC	42	BC	41	BC	40
	FA	60	5	65	BC	66	BC	66	BC	64	BC	65	BC	63
	AD	70	0.5	15	BC	15	BC	15	BC	16	BC	14	BC	14
ABG	AE	50	100	90	ABG	25	ABG	25	ABG	23	ABG	27	ABG	27
	AB	10	50	40	ABG	42	ABG	42	ABG	41	ABG	39	ABG	38
	AC	30	25	65	ABG	67	ABG	67	ABG	63	ABG	65	ABG	66
	FA	60	5	15	ABG	14	ABG	14	ABG	15	ABG	16	ABG	15
ACG	AD	70	0.5	90	ACG	89	ACG	89	ACG	90	ACG	88	ACG	91
	AE	50	100	25	ACG	26	ACG	27	ACG	25	ACG	24	ACG	25
	AB	10	50	40	ACG	39	ACG	39	ACG	42	ACG	42	ACG	43
	AC	30	25	65	ACG	63	ACG	63	ACG	64	ACG	65	ACG	65
BCG	FA	60	5	15	BCG	16	BCG	16	BCG	14	BCG	16	BCG	15
	AD	70	0.5	90	BCG	92	BCG	92	BCG	91	BCG	89	BCG	89
	AE	50	100	90	BCG	92	BCG	90	BCG	90	BCG	90	BCG	90
	AB	10	50	25	BCG	25	BCG	25	BCG	25	BCG	25	BCG	25
ABC	AC	30	25	40	ABC	42	ABC	40	ABC	43	ABC	40	ABC	40
	FA	60	5	65	ABC	64	ABC	65	ABC	65	ABC	65	ABC	65
	AD	70	0.5	15	ABC	16	ABC	15	ABC	15	ABC	15	ABC	15
	AE	50	100	90	ABC	91	ABC	90	ABC	89	ABC	90	ABC	90
	AB	10	50	25	ABC	24	ABC	25	ABC	24	ABC	25	ABC	25
ABCG	AC	30	25	40	ABCG	42	ABCG	40	ABCG	39	ABCG	41	ABCG	40
	FA	60	5	65	ABCG	66	ABCG	64	ABCG	63	ABCG	67	ABCG	65
	AD	70	100	15	ABCG	14	ABCG	16	ABCG	15	ABCG	17	ABCG	15
	AE	50	100	90	ABCG	89	ABCG	90	ABCG	92	ABCG	93	ABCG	90
	AB	10	50	25	ABCG	25	ABCG	26	ABCG	25	ABCG	24	ABCG	25

5 Performance of the Method

To examine the proposed method in the test microgrid, different types of faults were simulated with different conditions in terms of the location of faults, arc

resistance, and type of faults. Using the suggested method distance and category of simulated faults are obtained and presented in Table 2. According to the results in Table 2, the suggested algorithm operates accurately in different fault conditions.

Fault resistance and high impedance fault conditions: Due to the simulation results in Table 2, the suggested method detects, locates, and classifies several faults with various arc resistance very accurately. Additionally, to investigate the high impedance condition several faults with 500 and 1000 Ω fault resistance are simulated. The presented method has good performance in high impedance fault detection and classification.

Sampling frequency: The signals of currents and voltages are digitalized by various sampling frequencies between 0.5-20 kHz. The results are in Table 2. The proposed approach's precision and accuracy are not changed with sampling frequency variation.

Noise effect: The measured signals are populated by Gaussian noise with SNR between 10-60%. The performance of the presented method has negligible changes with the different signal-to-noise ratios.

6 Conclusions

This paper proposes a new intelligent approach to locating and classifying faults in AC microgrids. The suggested technique decomposes the current and voltage signals by the dynamic decomposition method. The measures on the ℓ_p -norms are applied to resultant signals from the DDM. These measures become the features of a topology data analysis-based machine learning method. The presented technique is tested in signals on a test ac microgrid in noisy conditions, sampling frequency, and fault resistance variations and have high impedance fault condition with high performance. The data needed in the suggested algorithm is only a 100 μ s window which is remarkably smaller than most existent methods. This approach is shown to have a precision of 100% in the classifying mission and forecasting the error of approximately 20m for the fault location mission. The mean error of fault location is near 60% of the one reference for the power grid. Importantly the suggested approach operates properly in any AC microgrid, regardless of network topology.

Appendix

Table A1 Test system lines data.

	Resistance	Inductance	Voltage
Overhead line	120 m Ω /km	0.23 mH/km	11 kV
Cable	100 m Ω /km	0.15 mH/km	380 V

Table A2 Test system generation data.

	Nominal power	Voltage
Wind	20 kW	0.4 kV
Diesel generator	12 kVA	11 kV
Photovoltaic	80 kW	11 kV
Main AC grid	5 MVA	11 kV
Battery	20 kW	11 kV

Table A3 Test system transformers data.

	Nominal power	HV side Voltage	LV side Voltage
Between A and C	500 kVA	11 kV	400 V
Between E and F	8 MVA	11 kV	380 V

Intellectual Property

The authors confirm that they have given due consideration to the protection of intellectual property associated with this work and that there are no impediments to publication, including the timing of publication, with respect to intellectual property.

Funding

No funding was received for this work.

CRedit Authorship Contribution Statement

M. Dodangeh: Idea & conceptualization, Research & investigation, Methodology, Software and simulation, Revise & editing. **N. Ghaffarzadeh:** Supervision.

Declaration of Competing Interest

The authors hereby confirm that the submitted manuscript is an original work and has not been published so far, is not under consideration for publication by any other journal and will not be submitted to any other journal until the decision will be made by this journal. All authors have approved the manuscript and agree with its submission to "Iranian Journal of Electrical and Electronic Engineering".

References

- [1] A. Hooshyar and R. Iravani, "Microgrid protection," *Proceedings of the IEEE*, Vol. 105, No. 7, pp. 1332–1353, Jul. 2017.
- [2] A. Saber, H. H. Zeineldin, T. H. M. EL-Fouly, and A. Al-Durra, "A new fault location scheme for parallel transmission lines using one-terminal data," *International Journal of Electrical Power & Energy Systems*, Vol. 135, p. 107548, 2022.
- [3] T. E. Sati and M. A. Azzouz, "Optimal Protection Coordination for Inverter Dominated Islanded Microgrids Considering N-1 Contingency," *IEEE Transactions on Power Delivery*, Vol. 37, No. 3, pp. 2256–2267, 2022.
- [4] Y. Liang, L. Jiang, H. Li, G. Wang, Q. Zhong, and L. Wang, "Fault analysis and traveling wave protection based on phase characteristics for hybrid multi terminal HVDC systems," *IEEE Journal of Emerging and Selected Topics in Power Electronics*, Vol. 10, No. 1, pp. 575–588, 2022.
- [5] A. Osman and O. Malik, "Transmission line distance protection based on wavelet transform," *IEEE Transactions on Power Delivery*, Vol. 19, No. 2, pp. 515–523, 2004.
- [6] F. Namdari and M. Salehi, "High-speed protection scheme based on initial current traveling wave for transmission lines employing mathematical morphology," *IEEE Transactions on Power Delivery*, Vol. 32, No. 1, pp. 246–253, 2016.

- [7] V. Veerasamy, N. I. A. Wahab, M. L. Othman, S. Padmanaban, K. Sekar, R. Ramachandran, H. Hizam, A. Vinayagam, and M. Z. Islam, "LSTM recurrent neural network classifier for high impedance fault detection in solar PV integrated power system," *IEEE Access*, Vol. 9, pp. 32672–32687, 2021.
- [8] F. Wilches-Bernal, A. Bidram, M. J. Reno, J. Hernandez-Alvidrez, P. Barba, B. Reimer, R. Montoya, C. Carr, and O. Lavrova, "A survey of traveling wave protection schemes in electric power systems," *IEEE Access*, Vol. 9, pp. 72949–72969, 2021.
- [9] N. Zhang and M. Kezunovic, "Transmission line boundary protection using wavelet transform and neural network," *IEEE Transactions on Power Delivery*, Vol. 22, No. 2, pp. 859–869, 2007.
- [10] X. Magagula, Y. Hamam, J. Jordaan, and A. Yusuff, "Fault detection and classification method using DWT and SVM in a power distribution network," in *IEEE PES PowerAfrica*, pp. 1–6, 2017.
- [11] A. Yadav and A. Swetapadma, "Combined DWT and naive bayes based fault classifier for protection of double circuit transmission line," in *IEEE International Conference on Recent Advances and Innovations in Engineering (ICRAIE-2014)*, pp. 1–6, 2014.
- [12] M. Jimenez Aparicio, M. J. Reno, P. Barba, and A. Bidram, "Multi-resolution analysis algorithm for fast fault classification and location in distribution systems," in *IEEE International Conference on Smart Energy Grid Engineering (SEGE)*, pp. 1–7, 2021.
- [13] M. Mishra, R. R. Panigrahi, and P. K. Rout, "A combined mathematical morphology and extreme learning machine techniques based approach to micro-grid protection," *Ain Shams Engineering Journal*, Vol. 10, No. 2, pp. 307–318, 2019.
- [14] F. Wilches-Bernal, M. J. Reno, and J. Hernandez-Alvidrez, "A dynamic mode decomposition scheme to analyze power quality events," *IEEE Access*, Vol. 9, pp. 70775–70788, 2021.
- [15] P. J. Schmid, "Dynamic mode decomposition of numerical and experimental data," *Journal of Fluid Mechanics*, Vol. 656, pp. 5–28, 2010.
- [16] J. H. Tu, C. W. Rowley, D. M. Luchtenburg, S. L. Brunton, and J. N. Kutz, "On dynamic mode decomposition: Theory and applications," *Journal of Computational Dynamics*, Vol. 1, No. 2, pp. 391–421, 2014.
- [17] J. N. Kutz, S. L. Brunton, B. W. Brunton, and J. L. Proctor, *Dynamic mode decomposition: data-driven modeling of complex systems*. Society for Industrial and Applied Mathematics, 2016.
- [18] M. Ghotbi-Maleki and R. Mohammadi Chabanloo, "New computational method for optimal allocation of fault current limiters in power systems," *Iranian Journal of Electrical and Electronic Engineering*, Vol. 17, No. 4, pp. 1733–1733, 2021.
- [19] A. Bahmanyar, H. Borhani-Bahabadi, and S. Jamali, "Fault location in active distribution networks using improved whale optimization algorithm," *Iranian Journal of Electrical and Electronic Engineering*, Vol. 16, No. 3, pp. 302–312, 2020.
- [20] N. Dodangeh and N. Ghaffarzadeh, "A new fast and accurate fault location and classification method on MTDC microgrids using current injection technique, traveling-waves, online wavelet, and mathematical morphology," *Iranian Journal of Electrical and Electronic Engineering*, Vol. 16, No. 2, pp. 248–258, 2020.
- [21] C. H. Noh, C. H. Kim, G. H. Gwon, and Y. S. Oh, "Development of fault section identification technique for low voltage DC distribution systems by using capacitive discharge current," *Journal of Modern Power Systems and Clean Energy*, Vol. 6, No. 3, pp. 509–520, Jun. 2018.
- [22] S. Augustine, M. J. Reno, S. M. Brahma, and O. Lavrova, "Fault current control and protection in a standalone DC microgrid using adaptive droop and current derivative," *IEEE Journal of Emerging and Selected Topics in Power Electronics*, Vol. 9, No. 3, pp. 2529–2539, 2020.
- [23] A. Geron, *Hands-on machine learning with Scikit-Learn, Keras, and TensorFlow: Concepts, tools, and techniques to build intelligent systems*. O'Reilly Media, 2019.
- [24] B. Singh and S. Kumar, "Distributed incremental adaptive filter controlled grid interactive residential photovoltaic-battery based microgrid for rural electrification," *IEEE Transactions on Industry Applications*, Vol. 56, No. 4, pp. 1414–1423, 2020.
- [25] Y. Singh, W. Jons, J. E. Eaton, J. D. Sobek, J. Jagtap, G. M. Conte, E. G. Fuemmeler, K. Zhang, Y. Wei, D. V. V. Garcia, and B. J. Erickson, "A new TDA-based machine learning classifier framework for predicting hepatic decompensation from MR images," *Medical Imaging 2022: Imaging Informatics for Healthcare, Research, and Applications*. Vol. 12037, pp. 117–121, 2022.

- [26] H. Riihimäki, W. Chachólski, J. Theorell, J. Hillert, and R. Ramanujam, "A topological data analysis based classification method for multiple measurements," *BMC Bioinformatics*, Vol. 21, No. 1, pp. 1–18, 2020.
- [27] S. Choe and S. Ramanna. "Cubical homology-based machine learning: An application in image classification," *Axioms*, Vol. 11, No. 3, p. 112, 2022.
- [28] S. Kumar and B. Singh. "Dual-mode control of utility interactive microgrid," *IET Renewable Power Generation*, Vol. 14, No. 5, pp. 845–855, 2020.



M. Dodangeh received the B.Sc. degree in Electrical Engineering from the University of Zanjan, Zanjan, Iran, in 2011, the M.Sc. and Ph.D. degree in Electrical Engineering from Imam Khomeini International University, Qazvin, Iran, in 2015 and 2022. He is a visiting professor of Electrical Engineering at Imam Khomeini

International University. His research interests include power system studies, such as applications of digital signal processing in power system protection, micro grids, digital protective relays, power system stability, and power system optimization problems.



N. Ghaffarzadeh is an Associate Professor of Electrical Engineering at Imam Khomeini International University. His special fields of interest include power system protection and transient in power systems. He is the author of seven books in the field of power systems. He is also the author and co-author of over 120 technical papers.



© 2022 by the authors. Licensee IUST, Tehran, Iran. This article is an open-access article distributed under the terms and conditions of the Creative Commons Attribution-NonCommercial 4.0 International (CC BY-NC 4.0) license (<https://creativecommons.org/licenses/by-nc/4.0/>).